Topological dynamics in a catalysis experiment

Sascha O. Firle,[1] Mario A. Natiello,[1] and Markus Eiswirth[2]
[1]*Department of Quantum Chemistry, Uppsala University, Box 518, S-751 20 Uppsala Sweden*
[2]*Fritz-Haber Institut, Max-Planck-Gesellschaft, Berlin, Germany*
(Received 8 May 1995)

A time series of the catalytical reaction of CO and O_2 on a Pt(110) surface is used to model the topological features of the underlying attractor by reconstructing unstable periodic orbits in a three-dimensional imbedding space. The orbits reveal that the template supporting the dynamics cannot be that of a Smale's horseshoe. Some of the computed orbits imply positive topological entropy, showing that the time series is chaotic.

PACS number(s): 05.45.+b, 82.65.Jv

I. INTRODUCTION

Topological descriptions of strange attractors in three-dimensional (3D) flows are based on the organization of unstable periodic orbits [1]. This information can be summarized in the form of a template [2], which describes the entanglement of the orbits in the flow. The description is "robust" both with respect to small changes in control parameters and to coordinate transformations.

The interesting result for practical applications is that the topological description can be used to analyze experimental time series, which can be imbedded in 3D space. Up to now, there appeared to be a contradiction between the vast amount of theoretically possible templates and those actually found in experimental data [1,3], which all reduced to the two-branched horseshoe template.

In this Brief Report we discuss an experimental time series recorded from a catalyzed chemical reaction, which presents a different behavior; namely, an orbit organization that is incompatible with that of a horseshoe template. We also assess that the data is chaotic and discuss the limitations of our approach.

II. ORIGIN OF DATA

Chaos has been observed in a number of catalytic systems under various conditions [4]. Here we examine the catalytic CO oxidation on a Pt(110) single crystal surface under isothermal, low-pressure conditions. This system was found to exhibit a very rich variety of oscillatory behavior, including a period-doubling cascade [5,6]. From the computation of metric properties it is found that near the accumulation point the system exhibits simple chaos (one positive Lyapunov exponent), while measurements away from it resulted in hyperchaos (more than one positive Lyapunov exponent) [7,8]. Here we concentrate on the first case. We analyzed a time series (file B from Refs. [7,8]) that was recorded by monitoring the work function of the surface with a Kelvin probe at a rate of 0.15 s. It consists of 4850 four-digit integers corresponding to about 12 min of measurement. Long-term recordings were hampered by the difficulty to guarantee constancy of the pressures [6]. The data exhibited an information dimension $D_1 = 2.35 \pm 0.03$ (nearest neighbor algorithm), a Kolmogorov entropy $K_1 = 0.09 \pm 0.02$ (computed from the marginal redundance [9]) and a Lyapunov exponent of 0.07 ± 0.01 (Sano-Sawada algorithm). These metric properties, however do not give information about the topological structure of an attractor. Rather, attractors with very similar characteristic measures can exhibit quite different qualitative features.

III. TOPOLOGICAL ANALYSIS

The main assumption underlying our analysis is that the recorded data actually samples a finite portion of the attractor associated to a yet unknown dynamical system that can describe the data. The validity of this assumption has to be gauged at all stages of the procedure.

If the attractor is not a fixed point, periodic orbit, or quasiperiodic orbit, but rather it has an irregular, though recurrent behavior, we are likely to expect that part of it will consist of an infinite number of unstable periodic orbits, such as it happens with, e.g., the chaotic Lorenz attractor. We will first attempt to identify some of these orbits and later imbed them in a larger space where the minimal dynamical requirements are satisfied.

A. Close returns

We can estimate which periodic orbits are "sampled" by our time series with the method of close returns [10]. If a portion x_l, x_{l+1}, ..., x_{k-1} of our data were exactly a periodic orbit, then the values x_k, x_{k+1}, x_{k+2}, etc., would equal x_l, x_{l+1}, x_{l+2}, etc., respectively. Since we are sampling unstable periodic orbits together with unavoidable sampling errors, the equality will never be fulfilled in practice. At most, we can expect that

$$\frac{1}{N}\sum_{j=0}^{N-1} |x_{l+j} - x_{k+j}| < \epsilon. \tag{1}$$

We will consider that a portion of a time series is a candidate for a periodic orbit when the equation above is satisfied for ϵ small enough (usually of the order of a few percent of the standard deviation of the data) and N of the order of a few periods.

After filtering the initial data to achieve both high-frequency and low-frequency noise reduction, we identified 40 periodic orbits, most of them of period 3 or 6.

B. Imbedding

The main goal of an imbedding is to produce a multidimensional time series that can be regarded as a model of the flow of a dynamical system. In simpler words, it has to be free from self-intersections, because a dynamical flow cannot intersect itself, due to the unicity of the solutions of the differential equations that describe it. We estimated the self-intersection statistics by sampling the number of times that the cosine of the angle between the tangent directions of close-lying portions of the flow falls below a threshold [11]. A value of 1 for the cosine means that close-lying portions of the flow are parallel, reducing the chances of having a self-intersection. This criterion does not pick up a preferred imbedding; many 3D sets of coordinates may work equally well.

We encountered that in the 3D imbedding described below over 99% of the data gives a cosine value above 1/2. We have chosen the following set of coordinates based also on the fact that they do not corrupt the signal to noise ratio (as a derivative imbedding would) and that they yield a smooth imbedding:

$$x_1(k) = x(k), \tag{2}$$

$$x_2(k) = e^{-\tau} x_2(k-1) + x(k), \quad \text{with } x_2(0) = 0, \tag{3}$$

$$x_3(k) = \mathcal{H}[x](k) = \mathcal{F}^{-1}[\sqrt{2\pi}\, i\, \mathcal{F}[x]](k), \tag{4}$$

where we choose $\tau > 0$ such that $0 < e^{-\tau} < 1$. The coordinate x_2 is optimal for $e^{-\tau} = 0.99$ and it corresponds to a discretized integral of the dataset times a cutoff factor [1], since we have that

$$x_2(k) = \sum_{j=1}^{k} x(j) e^{-\tau(k-j)} \approx \int_0^{t_k} x(s) e^{-\tau(t_k - s)} ds. \tag{5}$$

Concerning x_3, $\mathcal{F}$ represents (a discretized implementation of) the Fourier transform. This coordinate is hence the (discretized version of the) Hilbert transform of the original set, i.e., the convolution of $x(t)$ with $g(t) = 1/t$:

$$\mathcal{H}[f](z) = \int_{-\infty}^{+\infty} \frac{x(t)}{t - z} dt. \tag{6}$$

Figure 1 shows a 2D projection of our 3D imbedding.

The inspection of the imbedded flow indicates that it is a good candidate for a dynamical model. Moreover, the structure of the flow admits the definition of a Poincaré section, and hence the analysis of the periodic orbits of the flow, now equipped with the 3D imbedding can be done in terms of the associated braids [1,12]. We also tested the assumption that the derived Poincaré map is 2D. A false-neighbors test [11] indicates that over 99% of the false neighbors (including data segments containing chaotic periodic orbits; see below) can be resolved with a 2D Poincaré map.

C. Template

The available data turned out to contain mainly period-3 and period-6 orbits. By following the orbits along the flow and taking their intersections with a set of transverse sections, we can identify the associated braid by inspection. In Fig. 2 we show two examples out of the 20 best identified orbits. Each braid crossing corresponds to portions of the periodic orbit that pass one above the other in the 3D flow. The crossings are described by generators or elementary crossings σ_i (σ_i^{-1}), where thread i passes over (under) thread $i+1$. The topological information present in a periodic orbit lies actually in its braid type [13,12]. Since the braid type is an equivalence class we rearranged the braid read from the flow to its simplest equivalent expression (compare Fig. 2 and Fig. 3 below).

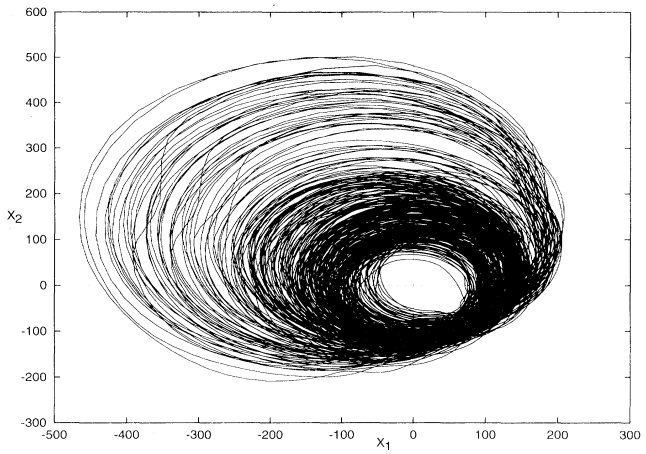

FIG. 1. 2D projection of the reconstructed flow.

The identification of a template amounts to specifying the number, ordering and folding of the branches that are necessary to host the encountered braid types. Since we only have knowledge of a finite number of periodic orbits via the close-return candidates, we can at most determine which is the minimum amount of branches which can host the observed orbits. An error in the determination of an orbit candidate may induce an error in the determination of the template. The error of our candidates is of the order of ϵ, i.e., the mismatch of the close returns. If two portions of the periodic orbit pass closer than ϵ to each other when they build an elementary crossing, we can actually not decide whether this crossing is σ_i or its inverse. To avoid this problem, we considered only the ca. 20 orbits, where the portions of the periodic orbit approached each other a distance larger than ϵ. The simplest template that can hold all of the identified orbits, and in particular those displayed in Fig. 2, is a three-branched template (see Fig. 3, where we include another, more entangled, period-6 orbit).

The candidate template need not be correct. Apart from holding the orbits, the template should render their linking properties. However a number of portions of the period-3 candidates passed closer than ϵ to the period-6. Hence, the linking numbers are determined with larger uncertainty than the braid types themselves. If we admit the computed linking numbers disregarding this uncertainty, we would need to add a fourth branch to our

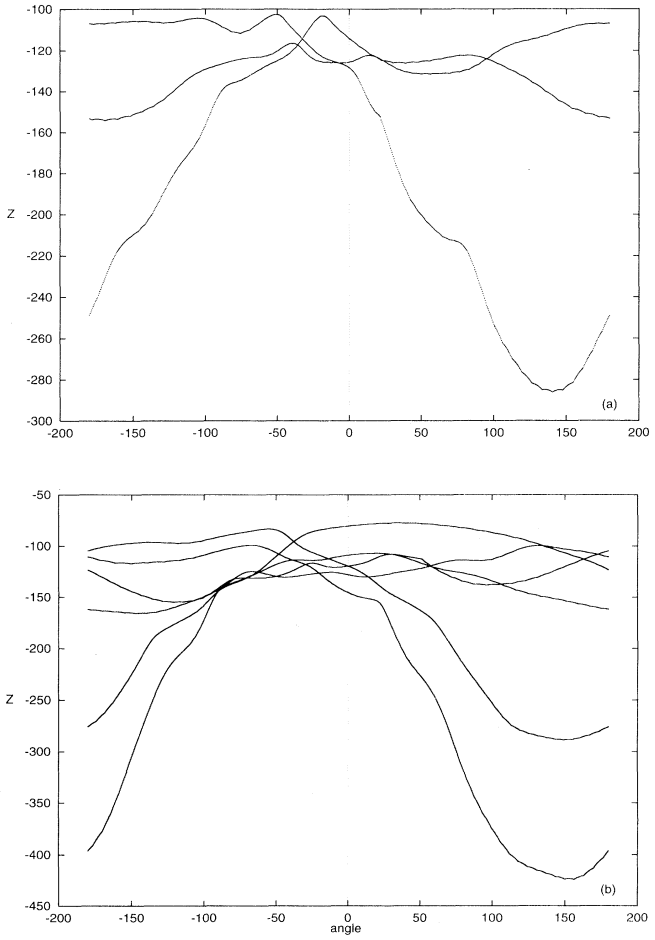

FIG. 2. Period-3 (a) and a period-6 (b) orbits as sampled from the imbedded flow. The abscissa denotes the angle ϕ at which the Poincaré section intersects the x-y plane, and the ordinate is the resulting new coordinate $z = \sin(\phi)x_1 + \cos(\phi)x_3$.

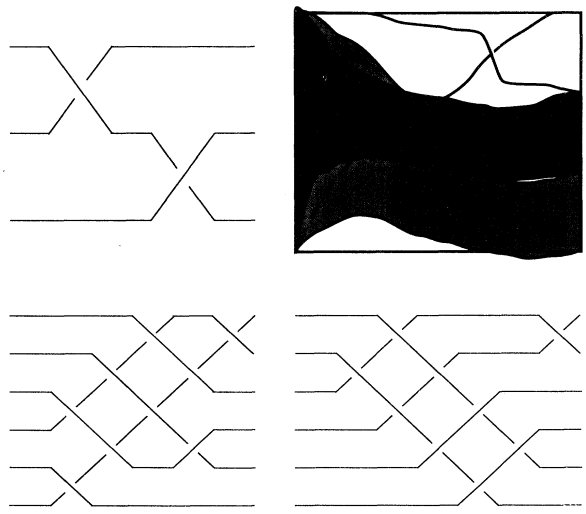

FIG. 3. Model template and the braid type of the period-3 and two period-6 orbits.

model template (or even a fifth branch depending on the degree of inaccuracy we are prepared to tolerate). In any case, our point is that the simplest template that is compatible with the data and the accuracy of the best periodic orbit candidates is that of Fig. 3. This template is complicated enough to assess our claim, i.e., that the data does not admit a horseshoe template. If the template were even more complicated, the result would still hold.

In a horseshoe template the folded branch, when regarded in such a way that the fold is counterclockwise as in Fig. 3, lands *in front of* the other branch. Hence, horseshoe orbits have a braid type that can be represented using only the braid generators σ_i and no inverse generator σ_i^{-1} [13]. No mixing of positive and negative exponents is present in the horseshoe braids. In contrast, our imbedded orbits have braid types with both the generators and their inverses, as seen in the examples. Since the folded branch of our model template falls *behind* the other branches, our model template is intrinsically in-

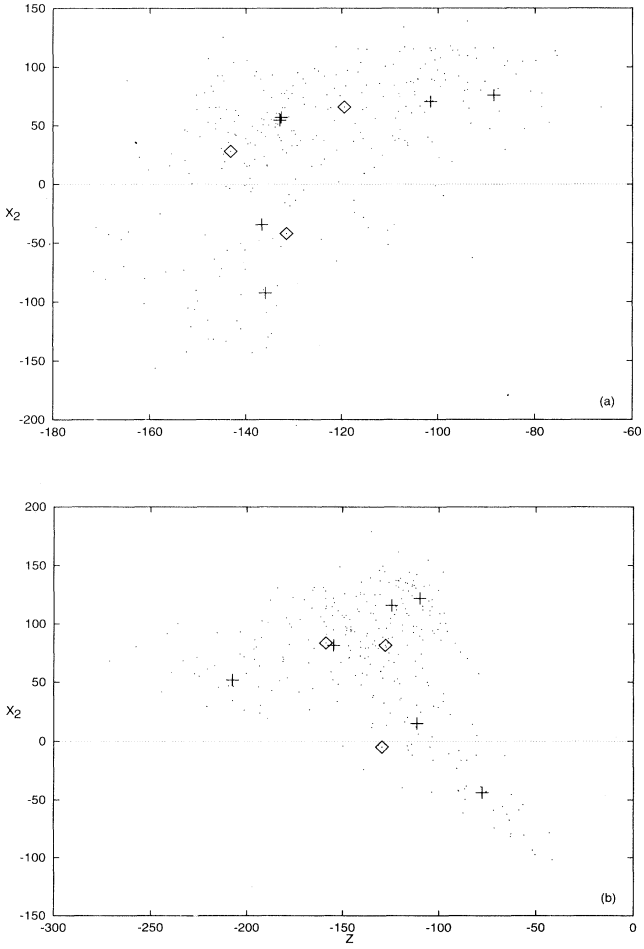

FIG. 4. View of two different choices of the Poincaré section for the adopted imbedding. The earlier referenced periodic orbits are marked with a cross (resp. a diamond). Coordinates are x_2 vs z (see Fig. 2), (a) $\phi = -80$, (b) $\phi = 39$.

compatible with a horseshoe template. This is the main result of this work.

D. Chaos and topological entropy

A 2D diffeomorphism having positive topological entropy is called *chaotic* [14]. It actually suffices to identify a periodic orbit of the diffeomorphism that implies positive entropy. In particular, the "badly ordered" period-3 orbit shown above implies positive entropy [15].

How can this strong theoretical result be confirmed in practice out of experimental data? Actually, it is not the periodic orbit itself, but rather the assumption that the orbit pertains to a 2D diffeomorphism that allows us to draw conclusions about entropy implication. If the diffeomorphism has a given orbit, by continuity it has to fold and stretch its domain in such a way that we can estimate bounds for the topological entropy. It is therefore crucial that the candidate orbits we obtain effectively sample the Poincaré map associated with the proposed imbedding [11]. This important fact has been overlooked until recently.

Since we have a finite data set, we can at most obtain a finite sampling of the Poincaré surface. To the extent that this sampling covers the surface, we can be confident that the identified orbits are characteristic of the Poincaré map and hence relevant to determine entropy and chaoticity. In such a case, the information we obtain can be reasonably ascribed to the experimental data.

If, on the other hand, our sampling consisted of a set of disjoint regions on the Poincaré surface, different imbeddings could yield different linkings *among* the regions. Information obtained from this linking is artificial; it depends on the imbedding and it cannot be ascribed to the data. It is therefore not relevant for the assessing of characteristic orbits [11]. In Fig. 4 we show how our data samples the Poincaré surface. It can be seen that the sampling is reasonably good, since together with the selected orbits, other points in the surrounding of the orbits are mapped along by the stretching and folding so that we can safely accept our example orbits to be representative of the behavior of the Poincaré map. We can therefore declare the data set to be chaotic. Note that this conclusion can be reached without invoking any metric properties.

IV. CONCLUDING REMARKS

Our two main results are that the dataset is chaotic because of the existence of a badly ordered period-3 orbit, and that it responds to a minimal template that is incompatible with the horseshoe template.

Having a nonhorseshoe template has definite consequences in the type of periodic orbits one encounters in the data, since horseshoe templates only have periodic orbits that can be represented by *positive* braids, i.e., braids consisting only of positive crossings σ_i.

The reliability of the results was established in several stages. Orbit candidates were only taken into account if the recurrent parts of the dataset stayed close over a time of the order of 5 periods or more. The suitability of the imbedding was checked self-intersection and false-neighbors statistics. The braid types were determined using orbit candidates having small error as compared with the crossing distance. The sampling of the Poincaré section by the imbedded points was found to be satisfactory. These measures are, however, qualitative: rather than a sharp answer they give an estimate of how meaningful a result may be.

ACKNOWLEDGMENTS

We are grateful to R. Gilmore (Drexel University, Philadelphia, USA), who suggested the use of the Hilbert Transform and to H. Solari and G. Mindlin (University of Buenos Aires, Argentina) for fruitful discussions. Financial support from the Swedish Institute and the Deutscher Akademischer Austauschdienst (DAAD) is gratefully acknowledged.

[1] G. B. Mindlin *et al.*, J. Nonlinear Sci. **1**, 147 (1991).
[2] P. Holmes, in *New Directions in Dynamical Systems*, edited by T. Bedford and J. Swift (Cambridge University Press, Cambridge, 1988), p. 150.
[3] F. Papoff *et al.*, Phys. Rev. Lett. **68**, 1128 (1991).
[4] M. Eiswirth, in *Chaos in Chemistry and Biochemistry*, edited by R. J. Field and L. Györgyi (World Scientific, Singapore, 1993), p. 141.
[5] M. Eiswirth and G. Ertl, Surf. Sci. **177**, 90 (1986).
[6] M. Eiswirth, K. Krischer, and G. Ertl, Surf. Sci. **202**, 565 (1988).
[7] M. Eiswirth, T.-M. Kruel, G. Ertl, and F. W. Schneider, Chem. Phys. Lett. **193**, 305 (1992).
[8] T.-M. Kruel, M. Eiswirth, and F. W. Schneider, Physica D **63**, 117 (1993).
[9] T.-M. Kruel, Ph.D. Thesis, Julius-Maximilians-Universität, Würzburg, Germany, 1992 (unpublished).
[10] D. P. Lathrop and E. J. Kostelich, in *Measures of Complexity and Chaos*, Vol. 208 of *NATO Advanced Study Institute, Series B*, edited by N. B. Abraham, A. M. Albano, A. Passamante, and P. E. Rapp (Plenum, New York, 1989).
[11] B. G. Mindlin and H. G. Solari, Phys. Rev. E **52**, 1497 (1995).
[12] M. A. Natiello and H. G. Solari, J. Knot Theory Ramific. **3**, 511 (1994).
[13] T. Hall, Nonlinearity **7**, 861 (1994).
[14] A. Katok, Publ. Math. Inst. des Hautes Etud. Sci. **51**, 137 (1980).
[15] P. Boyland, Technical report, Department of Mathematics, Boston University (unpublished).

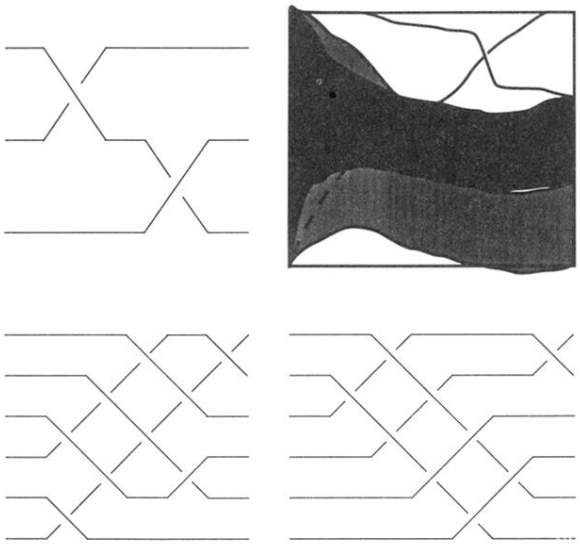

FIG. 3. Model template and the braid type of the period-3 and two period-6 orbits.